



Microstructure characterisation of alumina coating on steel by PEO

Y L Wang, M Wang, M Zhou, B J Li, G Amoako & Z H Jiang

To cite this article: Y L Wang, M Wang, M Zhou, B J Li, G Amoako & Z H Jiang (2013) Microstructure characterisation of alumina coating on steel by PEO, Surface Engineering, 29:4, 271-275, DOI: [10.1179/1743294412Y.0000000084](https://doi.org/10.1179/1743294412Y.0000000084)

To link to this article: <https://doi.org/10.1179/1743294412Y.0000000084>



Published online: 12 Nov 2013.



Submit your article to this journal [↗](#)



Article views: 120



View related articles [↗](#)



Citing articles: 10 View citing articles [↗](#)

Microstructure characterisation of alumina coating on steel by PEO

Y. L. Wang^{*1}, M. Wang¹, M. Zhou^{*1}, B. J. Li¹, G. Amoako¹ and Z. H. Jiang²

Alumina ceramic coating was prepared on Q235 carbon steel by plasma electrolytic oxidation. The discharge process was analysed according to the voltage–time curve. The microstructure of the ceramic coating was investigated by scanning electron microscopy, X-ray diffractometry and energy dispersive X-ray spectroscopy. The bonding strength, thickness, hardness, surface roughness and corrosion properties of the coatings were studied. The results indicated that coating on Q235 carbon steel mainly consisted of α -Al₂O₃ and γ -Al₂O₃. The coating showed coarse and porous surface. The surface roughness of the coating was 1.8 μ m, and the average diameter of the pores was 3–4 μ m. The hardness of the coating was 1854 HV. The thickness of the coating was \sim 28 μ m, and the bonding strength was 23 MPa. The corrosion tests indicated that the corrosion current density of alumina coated Q235 in 3.5%NaCl was 8.289×10^{-7} A cm⁻², which was decreased by two orders of magnitude compared with the uncoated one. The corrosion potential was increased to -0.379 V, which shifted positively by 0.303 V compared to the uncoated one.

Keywords: Alumina, Coating, Steel, Corrosion, PEO

Introduction

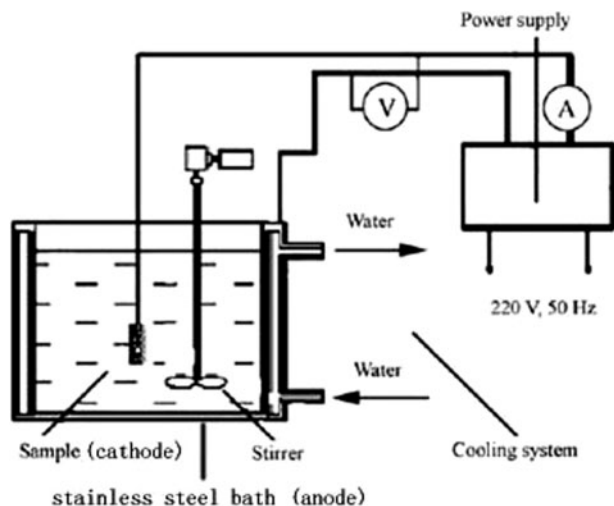
Plasma electrolytic oxidation (PEO), also known as microarc oxidation, is a relatively new technique in surface engineering fields. The PEO process is characterised by applying high electrical potential between the sample (usually anode) and a counterelectrode in liquid. Dielectric breakdown will take place near the sample surface and discharge occurs. Fast moving sparks can be seen on the sample surface. The temperature in the discharge channels can reach 10³–10⁴ K, and the pressure can reach 10²–10³ MPa.^{1,2} Many kinds of ceramic coatings with attractive properties such as wear resistance and corrosion resistance can be fabricated on the metal surface.^{3–5} However, as an effective technique, PEO cannot be used to treat steels directly. Of all the metals, steels are the most widely used materials in engineering. However, the performance of steels, especially the corrosion resistance of some steels, is not very good, which limits their application.⁶ According to previous work, only those metals^{7,8} such as Al, Mg and Ti (called valve metals) are suitable for PEO treatment. In fact, researchers have been in pursuit of preparing ceramic coating on ferrous metals by PEO since its emergence. Efforts have been made by McNiell and Nordbloom,⁹ McNiell and Gruss¹⁰ and Trovsky.¹¹

Recently, researchers succeeded in preparing ceramic coatings on steels with PEO, but pretreatments were usually needed. Valve metal was deposited on surface of steels before PEO treatment.^{12,13} Now, it is widely agreed that practical ceramic coatings on steels can hardly be achieved using a single PEO technique.¹⁴ Researchers also started to study the mechanism of PEO very early.⁴ Many mechanisms of the breakdown have been brought out, but none of them can explain all the experimental phenomena. However, it is also widely accepted by the researchers that the PEO process first depends on the nature of the metal, but the electrolyte and the power source also play very important roles. This provides a research direction for PEO treatment of both valve metals and steels in the future. Various electrolytes and several modes of power source have been adopted for PEO.^{15,16} Very recently, our researcher group attempted to apply PEO on carbon steel with a new mode of power source, and desirable results were obtained.¹⁷ In the present study, organic solution was exploited as the electrolyte, which is different from most of the universal electrolytes. In addition, the polarity of the metal in PEO treatment is also of great importance. Therefore, the PEO process here employs the sample as cathode. Alumina ceramic coating, which shows excellent properties among many ceramic coatings, was fabricated on carbon steel by PEO. The morphology, elemental and phase composition of the ceramic coatings were investigated. The bonding strength, thickness, hardness, surface roughness and corrosion resistance were also studied. Investigation indicated that the PEO in this study provided a promising technique for surface modification of carbon steels.

¹Center for Photon Manufacturing Science and Technology, School of Materials Science and Engineering, Jiangsu University, Zhenjiang 212013, China

²School of Chemical Engineering and Technology, Harbin Institute of Technology, Harbin 150001, China

*Corresponding authors, mzhou@ujs.edu.cn; wangyunlonghit@yahoo.com.cn



1 Schematic view of PEO system

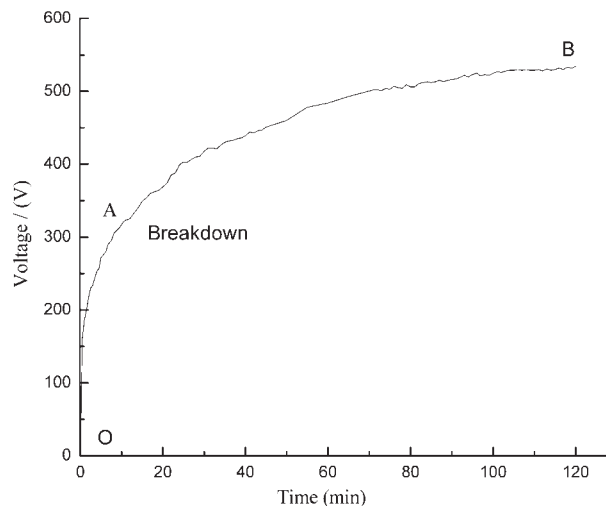
Experimental

Coating preparation

Q235 carbon steel with the composition of 0.14–0.22% C, 0.30–0.65% Mn, $\leq 0.30\%$ Si, $\leq 0.045\%$ P, $\leq 0.05\%$ S and Fe balance (all values are in wt-%) was processed into the size of $15 \times 1.5 \times 0.8$ mm. Samples were first polished and then cleaned before PEO treatment. The PEO experimental system contains a homemade single polar pulsed electrical power source and stainless steel electrobath. During the PEO process, the carbon substrate was used as cathode and the stainless steel electrobath served as anode. A PTFE stirrer was used and the running water around the stainless steel electrobath was used as cooling system to keep the electrolyte remain room temperature. The schematic view of PEO system is shown in Fig. 1. The electrolyte was the absolute ethanol solution of $\text{Al}(\text{NO}_3)_3 \cdot 9\text{H}_2\text{O}$ (18 g L^{-1}). The PEO process was carried out for 120 min under the stable current density of 8 A dm^{-2} . The frequency was 3000 Hz and the duty ratio was 45%.

Coating characterisation

The surface and cross-section morphology of the ceramic coating was investigated by a scanning electron microscope (SEM, Hitachi S-570); the phase and elemental composition were measured by X-ray diffractometer (XRD, D/max-rB, Japan, Cu target, K_α radial) and energy dispersive X-ray spectroscopy (EDS, Oxford Model 7537, UK), respectively. The bonding strength of the coating was determined using a direct pull-off test. The tested area was a circle with an area of 1 cm^2 . The thickness of sample was measured using an eddy current based thickness gauge (TT260, Time Company, China). The surface roughness of PEO coatings was tested by roughness tester (JB-4C, Shanghai, China). The microhardness of samples was evaluated by means of an MH-5 hardness tester using a Vickers indenter with the load of 100 g and for a dwelling time of 10 s. The corrosion tests were evaluated by potentiodynamic polarisation through a CHI604 electrochemical analyser in 3.5% NaCl solution with a sweeping rate of 0.167 mV s^{-1} .



2 Voltage-time curve during PEO process

Results and discussion

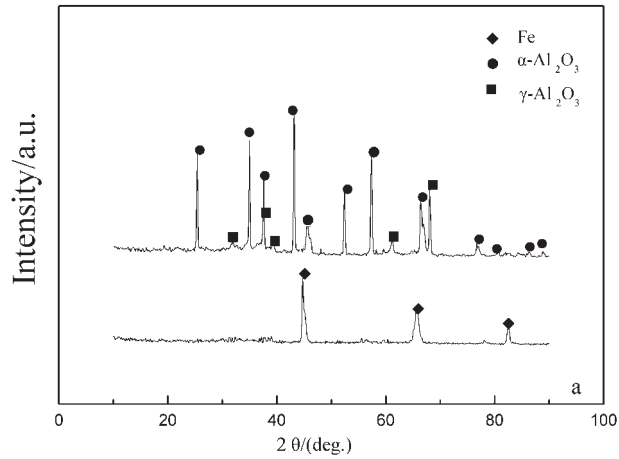
Discharge process analysis

Figure 2 shows the voltage-time curve during the PEO process. The curve shows a similar trend of that in universal PEO.¹ The PEO process can be roughly divided into two periods according to the inflection on the curve (separated by point A on the curve). In the first period, the voltage increased rapidly and the cathode surface was accompanied by many gas bubbles. Occurrence of the second period was characterised by the appearance of small white sparks on the sample surface. At first, these small sparks were rare but distributed uniformly. Later, the small sparks became denser and denser and gradually spread all over the sample surface. With increasing the treating time, the colour of the sparks changed from white to cyan, then blue and purple at last. When purple sparks appeared, the discharge points became fewer and the duration of discharge time at one point became a little longer. The discharge phenomenon in PEO was the breakdown of cathode including the breakdown of the barrier film and the gas.⁴

Microstructure and properties of coating

Phase and elemental composition of coating

The XRD and EDS spectra of the obtained coating are plotted in Figs. 3 and 4, respectively. Figure 3 shows that the coating is composed of $\alpha\text{-Al}_2\text{O}_3$ and $\gamma\text{-Al}_2\text{O}_3$. Comparing the spectra of the coating and substrate, it can be seen that no feature peaks of Fe are presented in the patterns. Therefore, it can be concluded that that no large amount of crystal Fe entered into the coating. It can also be supposed that the X-ray did not penetrate through the coating into the substrate, so no feature peaks of Fe from the substrate were found. In addition, low background of the XRD spectrum implies good crystallisation of the coating, which is a superiority to the some universal cathodic deposition techniques without discharges. In order to obtain crystal phase, a thermal treatment is usually needed for universal cathodic deposition technique.¹⁷ In addition, PEO treatment of steel reported here can obtain pure Al_2O_3 simply and directly compared to the indirect PEO treatment of steel reported in literature^{12,13}



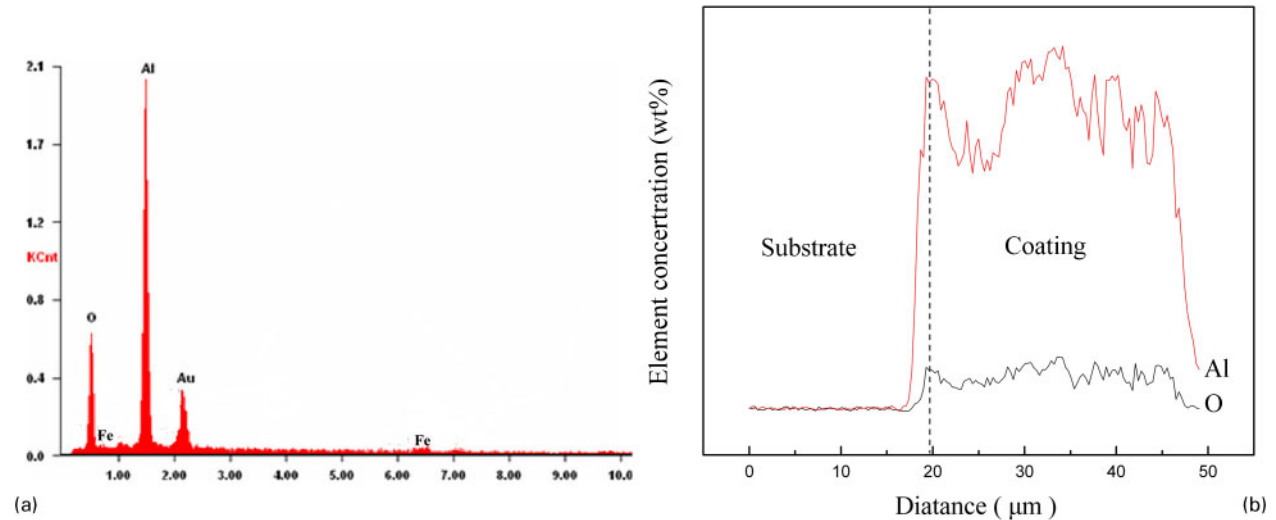
3 X-ray diffractometry patterns of PEO coating and carbon steel substrate

Al^{3+} in ethanol solution excited in the form of Al^{3+} and NO_3^- . During the PEO process, NO_3^- will be reduced and OH^- can be obtained.¹⁸ Aluminium hydroxide will be formed through the reaction of Al^{3+} and OH^- .⁴ Alumina will be formed from aluminium hydroxide during the plasma discharge reaction.^{19,20}

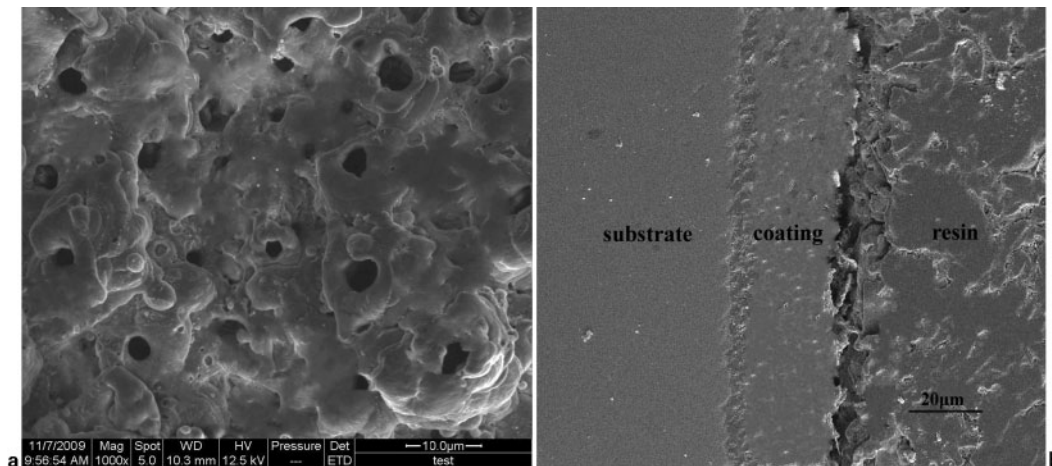
Surface EDS spectra in Fig. 4 represent that the coating is mainly comprised of Al and O and nearly no Fe is found. Au peak in the spectra results from the Au film deposited on the samples surface in SEM and EDS tests. The Au film is used to enhance the conductivity of the sample, and images with high quality can be obtained in SEM and EDS tests. In order to study the distribution regularity of Al and O elements, EDS spectra of the coating cross-section are shown in Fig 4b. A similar distribution tendency of Al and O is found, which agrees with the XRD analysis.

Surface and cross-section morphology of coating

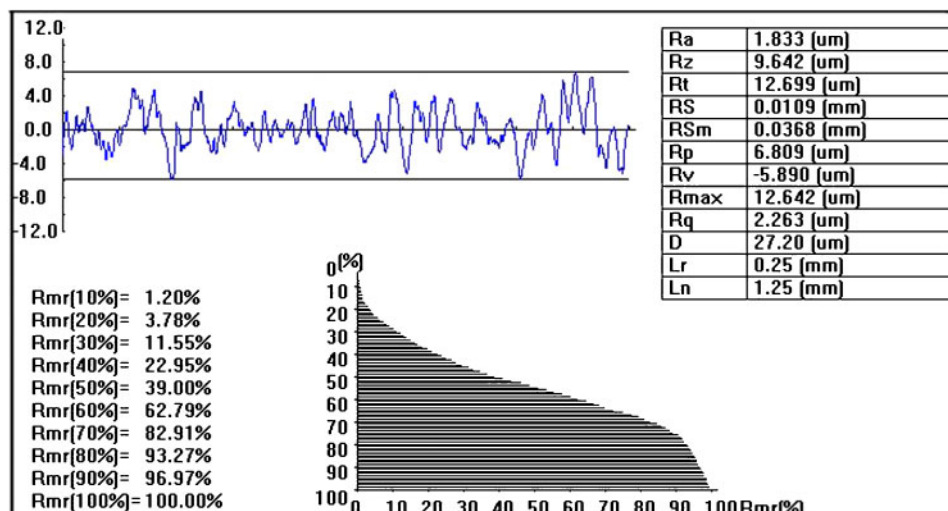
Figure 5 illustrates the surface and cross-section morphology of the PEO coating. Figure 5a exhibits that the coating surface also shows the volcanic morphology. The coating surface is coarse and porous and it is very similar to the coating surface of valve metal in universal PEO. It can be deduced that the ‘mouth’ of the volcano is the residual discharge channel during the discharge reaction. The irregular shaped areas around the volcanic mouth are formed due to the rapid cooling of the electrolyte. The average diameters of the pores are 3–4 μm . Figure 5b reveals that the cross-section of the



4 Energy dispersive X-ray spectroscopy patterns of PEO coating surface: a element distribution on surface; b element distribution on cross-section



5 Surface and cross-section morphology of obtained coating: a surface morphology; b cross-section morphology



6 Surface roughness test curve of Al_2O_3 PEO coating on Q235 carbon steel

coating is uniform and there is no evident discontinuity between the coating and the substrate.

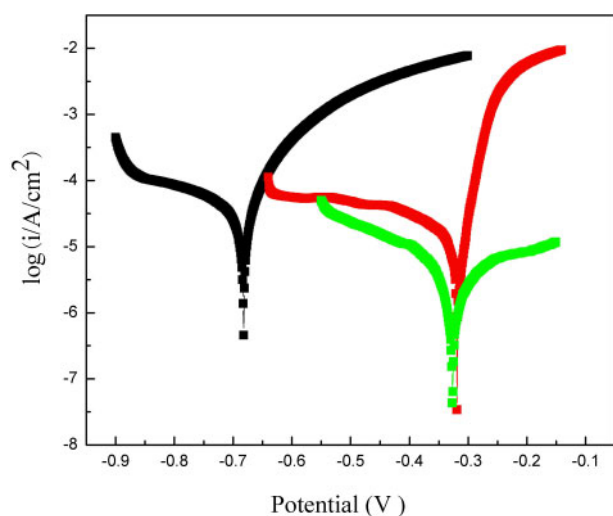
Properties of coating

The pull-off test indicated that the bonding strength was 23 MPa. This value is relatively high. The thickness test revealed that the thickness of the coating was 28 μm , which was also approved by the cross-section image in Fig. 4b.

Hardness tests reveal that the microhardness of Q235 carbon steel substrate and alumina ceramic coating was 413 and 1854 HV, respectively. The microhardness of the PEO coating was increased by more than four times as that of the uncoated substrate. High hardness of the coating was attributed to the existence of $\alpha\text{-Al}_2\text{O}_3$ in the coating.

The surface roughness test curve of Al_2O_3 PEO coating on Q235 carbon steel is shown in Fig. 6. It reveals that the surface roughness of the coatings was 1.8 μm . The surface roughness is relatively low compared to many PEO coatings on valve metals.¹

Figure 7 shows the polarisation curves of the samples with and without PEO coating. As a contrast, the polarisation curve of 0Cr18Ni9 stainless steel is also given. It can be seen that the coated sample possesses



7 Polarisation curves of samples

much higher corrosion potentials and lower corrosion current density than the uncoated one. The corrosion current density and corrosion potential of the uncoated Q235 substrate are $3.810 \times 10^{-5} \text{ A cm}^{-2}$ and -0.682 V respectively. For sample with PEO coating, the values are decreased to $8.289 \times 10^{-7} \text{ A cm}^{-2}$ and -0.379 V respectively. The corrosion current density is decreased by two orders of magnitude, and the corrosion potential shifts positively by 0.303 V. The better corrosion resistance of the coated steels is attributed to the chemical stability of the ceramic oxide coating, which can act as a barrier between the corrosion environment and substrate. Compared to 0Cr18Ni9 stainless steel, the sample with PEO coating shows rather close approximation corrosion resistance. Therefore, it can be concluded that the corrosion resistance of the carbon steel can be notably improved by PEO coating on the surface.

Conclusion

Alumina ceramic coating was prepared on Q235 carbon steel by PEO with the sample working as cathode. The alumina coating was composed of $\alpha\text{-Al}_2\text{O}_3$ and $\gamma\text{-Al}_2\text{O}_3$. The coating showed a little coarse and porous surface. The surface roughness of the coating was 1.8 μm , and the average diameter of the pores was 3–4 μm . The hardness of the coating was 1854 HV. The thickness of the coating was $\sim 28 \mu\text{m}$, and the bonding strength was 23 MPa. The corrosion resistance of the carbon steel could be significantly improved with alumina ceramic coating on the surface. The corrosion current density of alumina coated Q235 in 3.5%NaCl was $8.289 \times 10^{-7} \text{ A cm}^{-2}$, which was decreased by two orders of magnitude compared with the uncoated one. The corrosion potential was increased to -0.379 V , which shifted positively by 0.303 V compared to the uncoated one.

Acknowledgements

This work was financially supported by the Foundation for Advanced Talents of Jiangsu University (10JDG125), Open Fund of Jiangsu Provincial Key Laboratory of Tribology (KJSMCX2011006) and Natural Science Fund for Colleges and Universities in Jiangsu Province (11KJB430003).

References

1. A. L. Yerokhin, X. Nie and A. Leyland, A. Matthews and S. J. Dowey: *Surf. Coat. Technol.*, 1999, **122**, 73–93.
2. G. P. Wirtz, S. D. Brown and W. M. Kriven: *Mater. Manuf. Processes*, 1991, **6**, 87–115.
3. Y. H. Gu, C. F. Chen, S. Bandopadhyay, C. Y. Ning and Y. J. Guo: *Surf. Eng.*, 2012, **5**, 498–502.
4. M. A. Chen, N. Cheng, J. M. Li and S. Y. Liu: *Surf. Eng.*, 2012, **7**, 498–502.
5. Y. F. Jiang, Y. Y. Zhang, Y. F. Bao and K. Yang: *Wear*, 2011, **271**, (2), 1667–1670.
6. G. Sundararajan and L. Rama Krishna: *Surf. Coat. Technol.*, 2003, **167**, 269–277.
7. X. J. Li and B. L. Luan: *Mater. Lett.*, 2012, **86**, 88–91.
8. C. X. Ma, M. L. Zhang, Y. Yuan, X. Y. Jing and X. F. Bai: *Tribol. Int.*, 2012, **47**, 62–68.
9. W. McNiell and G. F. Nordbloom: US patent 2,854,390, 1958.
10. W. McNiell and L. L. Gruss: US patent 3,293,158, 1966.
11. I. Trovsky: US patent 2006016690-A1, 2006.
12. L. H. Lu, J. W. Zhang, D. J. Shen, L. L. Wu and G. R. Jiang: *J. Alloys Compd.*, 2012, **512**, 57–62.
13. Z. G. Huan, L. E. Fratila-Apachitei, I. Apachitei and J. Duszczky: *J. Funct. Biomater.*, 2012, **3**, 349–360.
14. W. C. Gu, G. H. Lv, H. Chen, G. L. Chen, W. R. Feng, G. L. Zhang and S. Z. Yang: *J. Alloys Compd.*, 2007, **430**, 308–312.
15. K. Wang, B.-H. Koo, C.-G. Lee, Y.-J. Kim, S.-H. Lee and E. Byon: *Trans. Nonferr. Met. Soc. China*, 2009, **19**, 866–870.
16. Z. P. Yao, D. L. Wang, Q. X. Xia, Y. J. Zhang, Z. H. Jiang and F. P. Wang: *Surf. Eng.*, 2012, **28**, 96–101.
17. X. Z. Yang, Y. H. He Ye, D. R. Wang and W. Gao: *Chin. Sci. Bull.*, 2003, **48**, 746–750.
18. L. Gal-Or, I. Silberman and R. Chaim: *J. Electrochem. Soc.*, 1991, **138**, 1939–1942.
19. W. Xue, Z. Deng, Y. Lai and R. Chen: *J. Am. Ceram. Soc.*, 1998, **81**, 1365–1368.
20. X. Nie, A. Leyland and H. W. Song: *Surf. Coat. Technol.*, 1999, **116–119**, 1055–1060.